THAUMASITE AS THE FINAL PRODUCT OF ALKALI-AGGREGATE REACTION: A CASE STUDY

M. Brouxel and A. Valiere*
DUNE Travaux Spéciaux, Centre d'Entreprise et d'Innovation, Campus Universitaire de la Doua, BP 2132, 69603 Villeurbanne Cedex, France

The AAR gels of two samples, studied with EDXA, present important variations of their SiO_2 (30 to 92%), CaO (7 to 68%), and Na_2O+K_2O (0.3 to 17%) contents. These variations, occurring over short distances (200 μm), are mainly related to the distance separating the gel from the aggregate: farther from the aggregate, the silicium content decreases and the calcium content increases. These AAR gels are intimately associated with massive sulfur enriched patches, showing also important chemical variations. Three components were defined in these patches: calcite, ettringite and thaumasite. The chemical trend existing between thaumasite and a silicium enriched component suggests that thaumasite is replacing the AAR gels. A transition between a massive sulfur enriched patch and AAR gel was observed confirming this hypothesis.

INTRODUCTION

In concrete affected by alkali-aggregate reactions (AAR), ettringite is often associated with the alkali-silica gel (Regourd et al (1), Regourd-Moranville (2)). Ettringite may even replace the gel (Jones and Poole (3), Jones (4)), especially for advanced reactions (Durand and Berard (5)).

In France, and particularly in the northern part of the country where most of the reactions were observed (Prin and Brouxel (6), Godart et al (7)), ettringite and alkali-silica gel are often associated (Deloye (8), Larive (9)). A possible raison for such association is the presence in the affected concretes, together with the reactive siliceous aggregates, of impure metamorphic limestones aggregates. The presence of pyrite, providing sulfur, and clay minerals, providing alumina, may explain the formation of ettringite in these samples (LeRoux and Toubeau (10, 11)).

In deteriorated concrete, thaumasite is commonly found associated with ettringite (Gouda et al (12), Lukas (13), Regourd et al (14), Lachaud (15), Crammond (16), Berra and Baronio (17)). Thaumasite, which has a formulae very similar to the one of ettringite, is commonly described as being formed from ettringite by substitution of Si for Al at very low temperature and high humidity ((13), (15), (16), (17), Van-Aardt and Visser (18)). Nonetheless, the association of thaumasite, ettringite and alkali-silica gel is rarely described ((1), Oberholster and Krüger (19)). Ettringite and thaumasite, forming often solid solutions ((12), Carpenter (20), Edge and Taylor (21, 22)) or discreet end-members ((15), Kollman, et al. (23)), is it possible to consider that some of the massive ettringite patches observed on aggregate surfaces are a mixture of ettringite and thaumasite. Moreover, it has been shown that thaumasite may be formed from silica gel (15). A close relationship between alkali-silica gel, ettringite, and thaumasite may therefore exist.

This paper presents the results of a scanning electron microscope (SEM) study conducted on concrete samples presenting, at the contact between the cement paste and the aggregates, AAR gels

* Université de Paris-Sud, Département des Sciences de la Terre, 91405 Orsay Cedex, France

but also massive ettringite and thaumasite patches. Energy dispersive X-Ray analysis (EDXA) coupled with the SEM were conducted on these AAR gels and sulfur enriched secondary products in order to define their relationships.

RESULTS

Twelve samples were collected on a 20 years old bridge presenting many signs of AAR: extensive surface cracking on all the structural members and gel exudation. Compared with a 1983 detailed inspection of this bridge, the number of cracks was multiplied by a factor ranging between 2.5 and 7 depending on the element, while the aperture of the cracks increased by a factor ranging between 1 and 4. These observations led to the conclusion that a continuing expansive phenomenon is taking place in this bridge.

Petrographic examination

The samples have been examined using a petrological microscope. Siliceous and calcareous aggregates were used in this concrete. The biggest aggregates are metamorphic siliceous limestones showing a strong foliation marked by oxides and sulfur minerals (pyrite). These limestones are similar to the Paleozoic limestones described in the Ardennes massif or near Boulogne (Debelmas (24), Soers and Meyskens (25)).

The smallest aggregates, more abundant (55 %), are siliceous aggregates. Small rounded quartz, undulatory extinction quartz and microcristalline quartz crystals have been observed. Dark reaction rims were often observed around the edges of the larger microcristalline quartz crystals. Moreover, these quartz crystals are often cracked, especially along their rims.

SEM and EDXA results

The SEM and EDXA results presented in this study come from two samples collected on the same concrete structural element: sample n°23 come from a part exposed to the rain while sample n°24 is from an area much more protected. The samples were observed and analyzed using a Hitachi scanning electron microscope coupled with a Link energy dispersive spectrometer. The analytical procedures followed in this study are similar to those reported in detail by Brouxel (26) and are briefly described in the paper by Remy and Brouxel ((27), this issue). The analytical errors used in this study are: $SiO_2 \pm 4$ %; $CaO \pm 1.1$ %; $Al_2O_3 \pm 2.3$ %, $MgO \pm 1.0$ %; $Na_2O \pm 1.2$ %; $FeO \pm 1.8$ %; $K_2O \pm 0.9$ %.

AAR gels were observed in both samples, sometimes associated with ettringite (Fig. 1, 2 and 3). These gels are usually located at the contact with the aggregates (Fig. 3). Massive ettringite and thaumasite patches have also been observed at the contact with the aggregates (Fig. 3 and 4).

AAR gel analyses. The AAR gels are chemically characterized by an important variation of their silicium, calcium and potassium contents (Table 1). These three elements represent around 100 % of the analyzed elements: $SiO_2 = 30$ to 92 %, $CaO = 7$ to 68 % and $Na_2O + K_2O = 0.3$ to 17 %. In a silicium versus calcium diagram these two elements, as already noted by Knudsen and Thaulow (28), are negatively correlated (Fig. 5). The two samples present gels with different chemical compositions: though, all the gel present important variations of their SiO_2 and CaO contents, gels of sample 23 present lower alkali contents (circles: $Na_2O + K_2O = 0.3$ to 5.5 %) compared to the gels of sample 24 (triangles: 1.5 to 17 %). This alkali enrichment is well described in the SiO_2 vs $Na_2O + K_2O$ diagram (Fig. 6): the gels show a maximum alkali enrichment for SiO_2 ranging between 40 and 60 %.

TABLE 1 - EDXA microanalyses of the AAR gels and sulfur enriched secondary products observed in the studied samples

Sample		Na2O	MgO	Al2O3	SiO2	S	Cl	K2O	CaO	FeO	Total	Na2O +K2O
23	aggregate	0,9	0,0	0,5	91,8	0,0	0,0	0,5	6,3	0,0	100,0	1,4
24	aggregate	0,5	0,0	0,0	95,4	0,0	0,0	0,8	3,2	0,1	100,0	1,3
23	cement paste	0,8	0,0	0,9	26,5	0,0	0,0	0,1	71,5	0,1	100,0	0,9
23	cement paste	0,1	1,0	5,5	24,6	0,0	0,1	0,4	67,9	0,4	100,0	0,5
23	cement paste	0,0	0,1	3,8	25,2	1,9	0,0	0,4	68,1	0,5	100,0	0,4
24	cement paste	0,0	0,8	3,1	9,3	3,9	0,0	0,7	81,6	0,6	100,0	0,7
24	cement paste	0,0	0,0	1,7	20,8	0,0	2,3	1,8	73,2	0,2	100,0	1,8
23	gel	0,0	0,5	1,3	42,4	0,0	0,1	0,8	54,7	0,2	100,0	0,8
23	gel	0,0	0,1	0,9	37,8	0,0	0,0	3,6	57,7	0,0	100,0	3,6
23	gel	0,8	0,1	0,0	88,2	0,0	0,2	0,2	10,6	0,0	100,0	1,0
23	gel	0,0	0,0	0,0	71,8	0,0	0,0	3,4	24,8	0,0	100,0	3,4
23	gel	0,3	0,0	0,2	84,0	0,0	0,0	1,4	14,0	0,1	100,0	1,7
23	gel	0,8	0,0	1,8	40,5	0,0	0,2	3,7	52,8	0,3	100,0	4,5
23	gel - layer 1	0,2	0,0	0,0	76,6	0,0	0,1	0,1	23,0	0,1	100,0	0,3
23	gel - layer 1	0,0	0,3	0,6	76,6	0,0	0,0	0,9	21,7	0,0	100,0	0,9
23	gel - layer 1	0,0	0,0	0,0	71,8	0,0	0,0	3,4	24,8	0,0	100,0	3,4
23	gel - layer 1	0,8	0,1	0,0	88,2	0,0	0,2	0,2	10,6	0,0	100,0	1,0
23	gel - layer 1	0,9	0,1	0,4	68,9	0,0	0,2	0,9	28,7	0,0	100,0	1,9
23	gel - layer 1	0,0	0,0	0,0	54,5	0,0	0,0	5,1	40,4	0,0	100,0	5,1
23	gel - layer 1	0,0	0,1	0,1	65,3	0,0	0,0	0,9	33,4	0,2	100,0	0,9
23	gel - layer 1	0,0	0,0	2,1	48,7	0,0	0,1	5,3	43,7	0,1	100,0	5,3
23	gel - layer 1	0,0	0,0	0,2	53,6	0,0	0,0	3,8	42,3	0,0	100,0	3,8
23	gel - layer 1	0,0	0,0	0,0	54,6	0,0	0,0	4,8	40,6	0,0	100,0	4,8
23	gel - layer 1	0,0	0,3	0,0	61,1	0,0	0,1	5,5	33,1	0,0	100,0	5,5
23	gel - layer 2	0,2	0,3	0,1	46,9	0,0	0,0	0,8	51,8	0,0	100,0	1,0
23	gel - layer 2	0,0	0,1	0,8	44,7	0,0	0,0	1,0	53,4	0,0	100,0	1,0
23	gel - layer 2	0,9	0,1	2,1	38,2	0,0	0,0	1,7	56,9	0,2	100,0	2,6
23	gel - layer 2	0,0	0,7	1,3	33,3	0,0	0,0	0,9	64,0	0,0	100,0	0,9
23	gel - layer 2	0,5	0,0	0,9	48,5	0,0	0,0	2,0	48,1	0,0	100,0	2,5
23	gel - layer 2	0,0	0,0	1,5	32,5	0,0	0,0	1,9	63,9	0,1	100,0	1,9
23	gel - layer 2	0,0	0,0	0,0	30,2	0,0	0,0	1,9	67,8	0,0	100,0	1,9
24	gel	1,2	0,7	1,0	48,7	0,0	0,0	15,7	32,4	0,2	100,0	16,9
24	gel	1,4	0,1	2,2	51,3	0,0	0,2	9,7	35,1	0,1	100,0	11,1
24	gel	2,7	0,3	0,0	64,9	0,0	0,0	10,9	20,9	0,3	100,0	13,5
24	gel	2,4	0,5	0,0	62,3	0,0	0,1	10,7	24,1	0,0	100,0	13,1
24	gel	0,2	0,0	0,0	91,5	0,0	0,0	1,3	7,0	0,0	100,0	1,5
24	gel	0,3	0,0	0,0	42,4	0,0	0,0	11,9	45,2	0,3	100,0	12,2
24	gel	0,3	0,0	0,3	40,2	0,0	0,0	11,3	47,5	0,2	100,0	11,7
24	gel	0,9	0,0	2,7	36,0	0,0	0,0	4,9	55,2	0,3	100,0	5,7
24	gel	0,5	0,7	1,4	34,5	0,0	0,0	1,8	60,7	0,5	100,0	2,2
24	gel	0,8	0,0	2,0	43,5	2,0	0,0	4,3	47,3	0,2	100,0	5,1
24	gel	1,1	0,3	2,1	39,4	0,0	0,0	10,7	45,7	0,8	100,0	11,8
23	ettringite	0,0	0,0	8,6	7,8	13,2	0,0	0,3	69,9	0,1	100,0	0,3
23	ettringite	0,2	0,0	9,0	4,1	14,8	0,0	0,3	71,3	0,3	100,0	0,5
23	ettringite-thaumasite	0,0	0,0	3,7	66,0	7,6	0,0	0,3	22,3	0,2	100,0	0,3
23	ettringite-thaumasite	0,0	0,0	0,8	0,8	0,7	0,1	0,0	97,3	0,3	100,0	0,0
23	ettringite-thaumasite	0,0	0,2	0,9	13,1	6,3	0,0	0,1	79,4	0,1	100,0	0,1
23	ettringite-thaumasite	0,5	0,0	8,4	0,0	7,5	0,0	0,0	83,7	0,0	100,0	0,5
23	ettringite-thaumasite	0,0	0,0	2,7	2,6	4,7	0,0	0,6	89,2	0,3	100,0	0,6
23	ettringite-thaumasite	0,0	0,6	6,5	1,0	0,0	0,0	0,0	91,3	0,6	100,0	0,0
23	ettringite-thaumasite	0,2	0,0	1,2	0,1	4,2	0,0	0,0	93,8	0,6	100,0	0,2
23	ettringite-thaumasite	0,1	0,0	9,9	0,3	15,8	0,0	0,3	73,6	0,1	100,0	0,4
23	ettringite-thaumasite	0,4	0,0	2,5	0,0	9,0	0,0	0,0	88,0	0,1	100,0	0,4
23	ettringite-thaumasite	0,2	0,0	10,9	0,0	14,6	0,0	0,1	74,2	0,1	100,0	0,4
23	ettringite-thaumasite	0,0	0,0	9,2	0,0	11,3	0,0	0,1	79,3	0,0	100,0	0,1
23	ettringite-thaumasite	0,0	0,0	5,4	2,7	12,4	0,0	0,0	79,6	0,0	100,0	0,0
23	ettringite-thaumasite	0,0	0,0	7,9	0,0	9,9	0,0	0,4	81,6	0,2	100,0	0,4
23	ettringite-thaumasite	0,5	0,0	5,3	0,7	9,1	0,0	0,1	84,3	0,0	100,0	0,7
23	ettringite-thaumasite	0,8	0,0	3,2	8,2	9,5	0,0	0,0	77,9	0,5	100,0	0,8
23	ettringite-thaumasite	0,4	0,0	1,4	1,5	10,5	0,0	0,0	86,1	0,2	100,0	0,4
23	ettringite-thaumasite	0,0	0,5	3,3	3,9	7,1	0,0	0,5	84,4	0,2	100,0	0,6
24	ettringite-thaumasite	0,0	0,0	10,2	23,4	12,6	0,0	0,3	53,5	0,0	100,0	0,3
24	ettringite-thaumasite	0,0	0,0	5,4	63,2	7,3	0,0	0,0	24,0	0,2	100,0	0,0
24	ettringite-thaumasite	1,3	0,0	14,7	13,2	11,6	0,0	0,8	58,0	0,5	100,0	2,1
24	gel-thaumasite	0,7	0,0	8,0	33,3	6,4	0,0	3,1	48,4	0,2	100,0	3,8

Two separate layers of gel (20 µm thick) were observed locally at the contact between the cement paste and an aggregate (Fig. 2). EDXA analyses were made on these two layers (Table 1). At the contact with the aggregate (gray circles), the gel is characterized by the following concentrations: SiO_2 = 49 to 88 %, CaO = 11 to 44 %, $Na_2O + K_2O$ = 0.3 to 5.5 %. Farther from the aggregate (open circles), the gel is characterized by lower SiO_2 and $Na_2O + K_2O$ concentrations but higher CaO concentrations: SiO_2 = 30 to 49 %, CaO = 48 to 64 %, $Na_2O + K_2O$ = 0.9 to 2.6%. These differences are well described in the SiO_2 vs CaO and SiO_2 vs $Na_2O + K_2O$ diagrams (Fig. 5 and 6). Therefore, even within the same layer of gel, important chemical variations exist.

The contact between an aggregate and the cement paste was studied in detail by Brouxel (29). The SiO_2, CaO and $Na_2O + K_2O$ contents are plotted against the distances separating the points (Fig 7 and Table 1). From the quartz aggregate to the cement paste, the silicium content decreases, while the calcium content increases. The alkali ($Na_2O + K_2O$) content is maximum within the reaction rim and shows lower values toward the quartz aggregate and the cement paste. It should be pointed out that most of the chemical variations occur at the contact with the aggregate: the alkali content increases rapidly at the contact with the aggregate and decreases slowly toward the cement paste. The SiO_2 content increases slowly from the cement paste to the aggregate, and, at the contact with the aggregate (≈ 100 µm) increases dramatically. On the other hand, the calcium content first decreases slowly, and then rapidly at the contact with the aggregate. The observed variations occurred over "large" distances and may not be influenced by any lateral spread effect. Indeed, the analytical points are separated by a minimum distance of 10 µm, while the lateral spread of the electrons in the micro-volume excited do not exceed 1 or 2 µm which agree with the theoretical and analytical values ((28), Diamond, et al (30)).

Massive ettringite and thaumasite patches. They have been observed, in both samples, at the contact between some aggregates and the cement paste (Fig. 3 and 4). Like the gel, they are characterized by important chemical variations: Al_2O_3 range from 1 to 15 %, SiO_2 from 0 to 66 %, S from 0 to 16%, and CaO from 24 to 97 % (Table 1; Fig. 9, 10). A transition between AAR gel and a massive ettringite and thaumasite patch was observed locally and studied in detail (Fig. 4 and Table 4). From the gel to the sulfur enriched secondary product, the following chemical variations were observed: decrease of the SiO_2 (44 to 13 %) and $Na_2O + K_2O$ (12 to 2 %) contents, and increase of the CaO (46 to 58 %), Al_2O_3 (2 to 15 %), and S (0 to 12 %) contents (Fig. 8).

DISCUSSION

This study enlighten the fact that AAR gels present important chemical variations even over short distances (200 µm). The silicium contents range between 30 and 90 % while the calcium contents range between 10 and 70 %. It seems that the element ruling these variations is the distance separating the gel from the reactive aggregate: close to the aggregate, the gel composition is enriched in silicium, while, farther from the aggregate, the gel composition is richer in calcium and very similar to the cement paste composition. Similar chemical trends have already been described by many authors ((1), (28), (29), Buck and Mather (31), Bérubé and Fournier (32), Diamond (33), Regourd (34)). These results showed also that there is likely a progressive chemical variation through the AAR gel, from the cement paste toward the reactive aggregate. The limit described previously between the two different observed gel layers can likely be placed at a distance of 100 to 150 µm from the aggregate; where a break occurs in the chemical trends (Fig.7).

The studied samples present abundant massive ettringite and thaumasite patches. Similar looking phases have been already described in the literature and are usually assigned to ettringite (e.g. (2)). It seems however that they present a complicated structure. Like the gel, they present important variation of their chemical composition (Fig. 9 and 10). Four components were defined: calcite, ettringite, thaumasite and quartz (all the analyses, but 5, plot in a triangle defined by calcite, ettringite and thaumasite). Nevertheless, it is noteworthy that no one analysis of true ettringite or thaumasite was obtained (the plotted points of ettringite and thaumasite were calculated from their

theoretical structural analyses). It is therefore likely that a solid solution exists between calcite, ettringite and thaumasite.

Moreover, five points plot between thaumasite and quartz. The silicium enrichment of these sulfur enriched massive patches (Fig. 9) argue for an origin from silica enriched product. Silicium is indeed necessary to produce thaumasite from ettringite at low temperature and high humidity ((13), (15), (16), (17), (18)). A possible origin for silicium is of course the abundant silica gels present in these samples. Such hypothesis agree with an experiment conducted by Lachaud (15) who synthesized thaumasite from silica gel at 1% aluminium content (calcite was always observed in the residues). The origin of the thaumasite from AAR gel is confirmed by the transition observed between the AAR gel and a massive ettringite and thaumasite patch (Fig. 4). It should be pointed out that calcite was always analyzed in these patches. Ettringite was likely to be originally associated with the now transformed AAR gel (e.g. Fig. 1). The sulfur necessary to form ettringite and thaumasite in these samples is likely to come either from the cement paste but more likely from the metamorphic limestones aggregates containing pyrite.

The relationships between the cement paste, the reactive aggregates, the AAR gel and the massive ettringite and thaumasite patches can be described in tertiary diagrams (Fig. 11). In the SiO_2 - CaO - $Na_2O + K_2O$ tertiary diagram, the gel of the two studied samples are well defined by their different alkali enrichments. Similarly, in the SiO_2 - CaO - S tertiary diagram the solid solution between calcite, ettringite and thaumasite, and the silicium enrichment are well described. Such diagrams may be very useful to describe all the components present in a deteriorated concrete.

CONCLUSION

Detailed chemical studies of AAR gels using a calibrated EDXA showed that gels present highly variable compositions. The following variations were recorded: SiO_2 = 30 to 92%, CaO = 7 to 68%, and Na_2O+K_2O = 0.3 to 17%. It appears that the main factor ruling these variations is the distance separating the gel from the reactive aggregate. Close to the aggregate, the gel is enriched in silicium; farther from the aggregate, the silicium content decreases and the calcium content increases (there is a negative correlation between silicium and calcium in the AAR gels). The alkali content shows a maximum somewhere in between the cement paste and the aggregate. It should be pointed out, that in real situations like this one, with no addition of alkalis and no acceleration of the reaction kinetics, only lime-alkali-silica gels are formed. This is an important difference with laboratory made gels which are more often alkali-silica gel. Close associations of gel and ettringite from one hand, and gel and massive sulfur enriched patches (ettringite + thaumasite + calcite) from the other hand were often observed in the studied samples. The massive sulfur enriched patches are, like the gel, characterized by important chemical variations : Al_2O_3 = 1 to 15%, SiO_2 = 0 to 66%, CaO = 24 to 97%, and S = 0 to 16%. They are likely constituted of a solid solution of three phases : calcite, ettringite and thaumasite. A transition between AAR gel and a massive sulfur enriched patch was observed suggesting that thaumasite was formed from the AAR gel following this non-equilibrated reaction: AAR gel + ettringite ——> thaumasite + ettringite + calcite. In this case, thaumasite represent the latest stage of the reaction that may occur only in speficic conditions (low temperature, high humidity, and presence of abundant sulfur).

REFERENCES

1. Regourd, M., Hornain, H., Mortureux, B. and Poitevin, P., 1981 "The alkali-aggregate reaction. Concrete microstructural evolution", Proceedings of the "5th International Symposium on Alkali-Aggregate Reaction in Concrete", Cape Town, South Africa.
2. Regourd-Moranville, M., 1989 "Products of reaction and petrographic examination", Proceedings of the "8th International Conference on Alkali-Aggregate Reaction", Kyoto, Japan.

3. Jones, T. N. and Poole, A. B., 1987 "Alkali-silica reactions in several U.K. concretes : the effect of temperature and humidity on expansion and the significance of ettringite development", Proceedings of the "7th International Conf. on AAR", Ottawa, Canada.
4. Jones, T. N., 1988, Chem. & Ind. 18, 40.
5. Durand, B. and Berard, J., 1987, Mat. & Struct. 20, 39.
6. Prin, D. and Brouxel, M., 1992 "Alkali-aggregate reaction in northern France : a review", Proceedings of the "9th International Conference on Alkali-Aggregate Reaction in concrete", London, England.
7. Godart, B., Fasseu, P. and Michel, M., 1992 "Diagnosis and monitoring of concrete bridges damaged by A.A.R. in northern France", Proceedings of the "9th International Conference on Alkali-Aggregate Reaction in concrete", London, England.
8. Deloye, F. X., 1989, Bull. liaison L.C.P.C. 161, 41.
9. Larive , C., 1990 " Les réactions de dégradations internes du béton. Où, quand, comment, pourquoi ?", L.C.P.C. Report OA-6.
10. LeRoux, A. and Toubeau, P., 1986 "Importance des minéraux accessoires des sols traités", Proceedings of the "XV Congr. Ass. Intern. Géologie de l'ingénieur (AIGI)", Buenos-Aires, Argentina.
11. LeRoux, A. and Toubeau, P., 1987 "Mise en évidence du seuil de nocivité et du mécanisme d'action des sulfures au cours d'un traitement à la chaux", Proceedings of the "IX Conf. de Géotechnique", Bangkok, Thaïlande.
12. Gouda, G. R., Roy, D. M. and Sarkar, A., 1975, Cem. & Conc. Res. 5, 519.
13. Lukas, W., 1975, Cem. & Conc. Res. 5, 503.
14. Regourd, M., Hornain, H., Mortureux, B., Bissery, P. and Evers, G., 1978, Ann. l'I.T.B.T.P. 358, 2.
15. Lachaud, R., 1979, Ann. l'I.T.B.T.P. 370, 2.
16. Crammond, N. J., 1985, Cem. & Conc. Res. 15, 1039.
17. Berra, M. and Baronio, G., 1989, ACI Spec. Pub. 100, 2073.
18. Van-Aardt, J. H. P. and Visser, S., 1975, Cem. & Conc. Res. 5, 225-232.
19. Oberholster, R. E. and Krüger, J. E., 1984 "Investigation of alkali-reactive, sulphide-bearing and by-product aggregates", Proceedings of the "International symposium on aggregates", Nice, France.
20. Carpenter, A. B., 1963, Amer. Min. 48, 1394.
21. Edge, R. A. and Taylor, H. F. W., 1969, Nature 224, 363.
22. Edge, R. A. and Taylor, H. F. W., 1971, Acta Cryst. B27, 594.
23. Kollman, H., Struebel, G. and Trost, F., 1977, Zem. Kalk Gips. 30, 224.
24. Debelmas, J., 1974, "Géologie de la France. Volume 1 : Vieux massifs et grands bassins sédimentaires", Doin, Paris, France.
25. Soers, E. and Meyskens, M., 1989 "Petrographical research on alkali-aggregate reactions in concrete structures in Belgium", Proceedings of the "Alkali-aggregate Reaction 8th International Conference", Kyoto, Japan.
26. Brouxel, M., 1991 "Energy dispersive X-Ray analysis (EDXA) : accuracy and reliability", Proceedings of the "3rd Euroseminar on microscopy applied to building materials", Barcelone,Spain.
27. Remy, P. and Brouxel, M., 1992 "Wollastonite : a reactive mineral to AAR", Proceedings of the "9th International Conference on Alkali-aggregate Reaction in concrete", London, England.
28. Knudsen, K. and Thaulow, N., 1975, Cem. & Conc. Res. 5, 443.
29. Brouxel, M., 1992, Cem. & Conc. Res., in press.
30. Diamond, S., Young, J. F. and Lawrence, F. V., 1974, Cem. & Conc. Res. 4, 899.
31. Buck, A. D. and Mather, K., 1978 "Alkali-silica reaction products from several concretes: optical, chemical and X-ray diffraction data", Proceedings of the "4th Int. Conf. Effects of Alkalis in Cement and Concrete", Purdue University, U.S.A.
32. Bérubé, M. A. and Fournier, B., 1986, Can. Miner. 24, 271.
33. Diamond, S., 1975, Cem. & Conc. Res. 5, 329.
34. Regourd, M., 1983, Ann. l'I.T.B.T.P. 59, 128-141.

DUNE Contribution Number 92/12

Figure 1 SEM micrograph of AAR gel associated with secondary ettringite

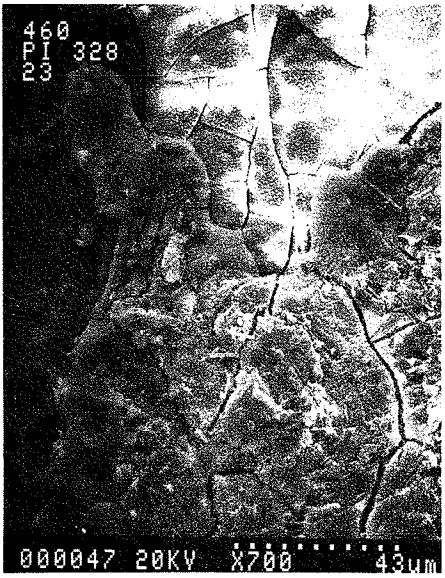

Figure 2 SEM micrograph of two separated gel layers

Figure 3 SEM micrograph of AAR gel associated with ettringite and thaumasite

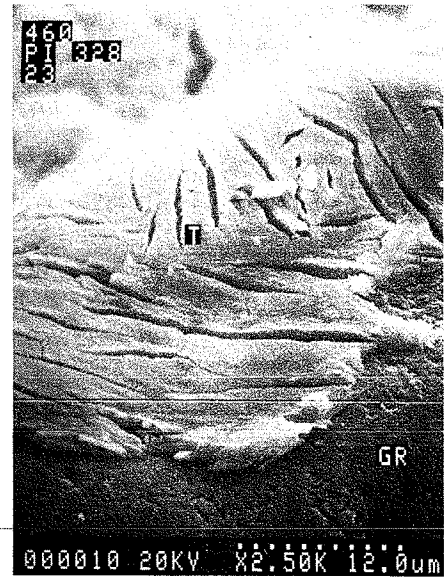

Figure 4 SEM micrograph of massive ettringite+ thaumasite + calcite patch on a reactive aggregate

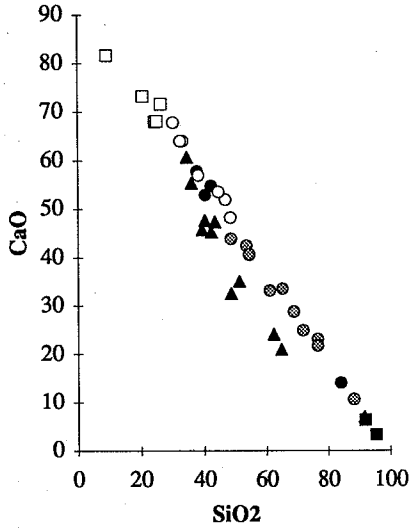

Figure 5 SiO_2 vs CaO graph

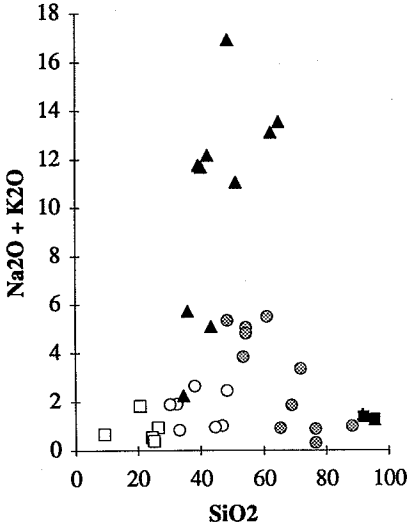

Figure 6 SiO_2 vs $Na_2O + K_2O$ graph

Open squares : cement paste; filled squares : quartz; circles : AAR gels sample 23 (gray circles : close to the aggregate, open circles : close to the cement paste); triangles : AAR gels sample 24.

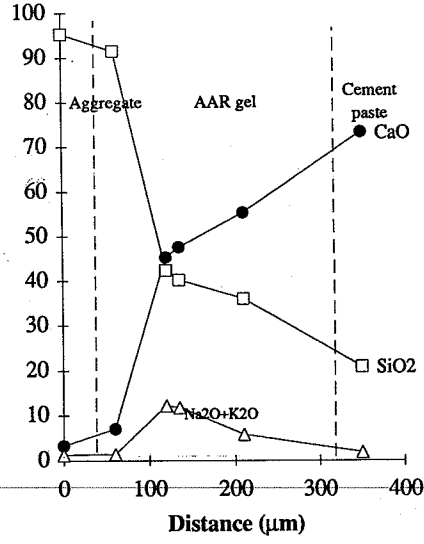

Figure 7 Variation of SiO_2, CaO and Na_2O $+K_2O$ from the aggregate to the cement paste

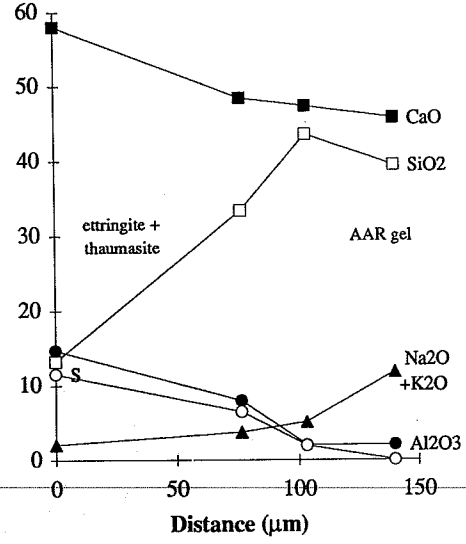

Figure 8 Variation of SiO_2, CaO, S, Na_2O+K_2O and Al_2O_3 from a gel to a sulfur enriched patch

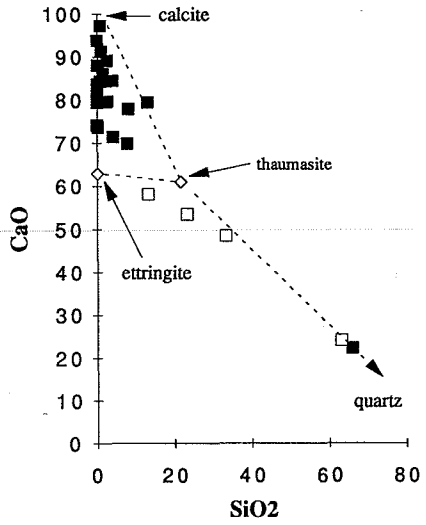

Figure 9 SiO_2 vs CaO graph

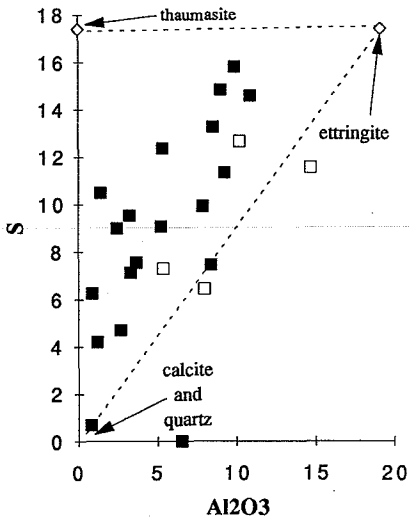

Figure 10 Al_2O_3 vs S graph

Ettringite + thaumasite + calcite massive patches : filled squares = sample 23; open squares = sample 24. The diamonds represent ettringite & thaumasite calculated points (structural formulae).

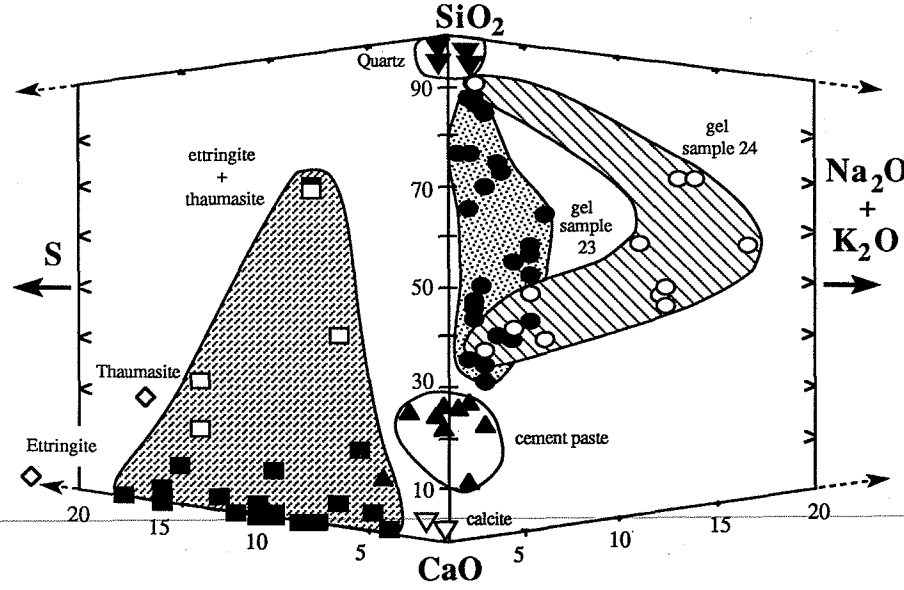

Figure 11 SiO_2-CaO-Na_2O+K_2O and SiO_2-CaO-S tertiary graphs for all the observed phases. Same symbols as above + quartz and cement paste: filled triangles and calcite: open triangles.